Research Square

Preprints are preliminary reports that have not undergone peer review.
They should not be considered conclusive, used to inform clinical practice,
or referenced by the media as validated information.

First Light Measurements Recorded by the Digital Absolute Radiometer Onboard the ESA PROBA-3 Mission

Jean-Philippe Montillet

jean-philippe.montillet@pmodwrc.ch

PMOD/WRC

Wolfgang Finsterle

PMOD/WRC

Daniel Pfiffner

PMOD/WRC

Margit Haberreiter

PMOD/WRC

Research Article

Keywords: Solar Irradiance, Instrumental Effects, Instrumentation and Data Management, Integrated Sun Observations, Solar Cycle, Observations

Posted Date: November 2nd, 2026

DOI: https://doi.org/10.21203/rs.3.rs-11316308/v1

License: This work is licensed under a Creative Commons Attribution 4.0 International License.
Read Full License

Additional Declarations: No competing interests reported.

First Light Measurements Recorded by the Digital Absolute Radiometer Onboard the ESA PROBA-3 Mission

Jean-Philippe Montillet[1] · **Wolfgang Finsterle**[1] · **Daniel Pfiffner**[1] · **Margit Haberreiter**[1]

© **The author(s)** ●●●●

Abstract We present the first light results from the Digital Absolute Radiometer (DARA) onboard the European Space Agency's PROBA-3 mission, launched on 5 December 2024. DARA-PROBA3 features three cavities that perform Total Solar Irradiance (TSI) measurements based on their component-level calibration. The uncertainty budget established before launch is revised in flight and extended with a dark correction derived from deep-space measurements, giving combined standard uncertainties of 181, 164 and 169 ppm for cavities A, B and C. First light was established on 25 February 2025, the three cavities recording 1362.15, 1362.02 and 1361.97 $\mathrm{W\,m^{-2}}$ at their respective first-measurement epochs. Averaged over their individual observation windows, DARA-PROBA3 gives a mean TSI of 1361.96 ± 0.09 $\mathrm{W\,m^{-2}}$ across the three cavities, in agreement with the value recorded by the VIRGO/PMO6 radiometer over the same interval (i.e. 1361.94 $\mathrm{W\,m^{-2}}$). Extending the analysis to the post-commissioning period, from August to October 2025, we identify two classes of instrumental outlier associated with the orbital geometry of the spacecraft. DARA-PROBA3 follows the VIRGO/PMO6 record at both minute and daily resolution, and shows the same sensitivity to solar fluctuations as DARA-JTSIM and TSIS-1/TIM at daily resolution, establishing a baseline for the mission.

✉ J.-P.M. Montillet
jean-philippe.montillet@pmodwrc.ch

W.F. Finsterle
wolfgang.finsterle@pmodwrc.ch

D.P. Pfiffner
daniel.pfiffner@pmodwrc.ch

M.H. Haberreiter
margit.haberreiter@pmodwrc.ch

[1] Physikalisch-Meteorologisches Observatorium Davos/World Radiation Center (PMOD/WRC), Davos Switzerland

Keywords: Solar Irradiance; Instrumental Effects; Instrumentation and Data Management; Integrated Sun Observations; Solar Cycle, Observations

1. Introduction

Total Solar Irradiance (TSI) is the integrated solar electromagnetic energy flux across the entire spectrum arriving at the top of Earth's atmosphere at the mean Sun–Earth distance of 1 AU. This fundamental solar parameter has been monitored continuously from space since 1978, forming one of the key parameters for understanding solar variability and its influence on Earth's radiation budget and climate forcing (Thuillier et al. 2006; Schmutz 2021). The nominal TSI value is 1361 W/m^2 as recommended by the IAU 2015 Resolution B (Prša et al. 2016). The long-term TSI record is essential for climate models and understanding the mechanisms linking solar variability to atmospheric and oceanic responses (Eyring et al. 2016; Egorova et al. 2018; Hansen et al. 2011; Kopp 2025). TSI is measured in space using electrical substitution radiometers (ESRs), cavity-based absolute instruments that rely on the principle of thermal equilibrium between absorbed solar radiation and dissipated electrical power (Suter 2014). The absolute calibration of these instruments determines the consistency and traceability of the global TSI database. Since the launch of the PREMOS/PICARD mission in 2010 (Schmutz et al. 2013), new TSI instruments have been calibrated on the system level against SI-traceable standards, particularly through the Total Solar Irradiance Radiometer Facility (TRF) at the Laboratory for Atmospheric and Space Physics (LASP), University of Colorado (Kopp et al. 2007; Montillet et al. 2026). Prior measurements, including the VIRGO/SOHO instruments launched in 1996, were calibrated relative to the World Radiometric Reference (WRR), which is itself offset from the SI scale by approximately 0.34% (Fehlmann 2011; Fehlmann et al. 2012).

The Project for On-Board Autonomy-3 (PROBA-3) is a European Space Agency formation-flying mission consisting of two spacecraft: the Occulter Spacecraft (OSC) and the Coronagraph Spacecraft (CSC). Launched the 5th of December 2024, PROBA-3 is designed primarily to achieve unprecedented high-resolution observations of the solar corona through external coronagraphy (Zhukov et al. 2026). The formation geometry and pointing stability required for coronagraph operations create an exceptionally stable solar-pointing platform with extended periods of uninterrupted solar viewing thanks to the long orbital period of 19.6 hours. The Digital Absolute Radiometer (DARA) radiometer is installed on the OSC (Figures 7 and 8, Appendix A). PROBA-3 follows a highly elliptical orbit ($600 \times 60\,530$ km, inclination $\approx 59°$, period $\approx$19.6 h), allowing continuous solar observation arcs of up to 19 hours (Montillet et al. 2026).

The DARA onboard PROBA-3 is the latest generation of electrical substitution radiometers developed by the Physikalisch-Meteorologisches Observatorium Davos and World Radiation Center (PMOD/WRC). DARA's design heritage traces through the Compact Lightweight Absolute Radiometer (CLARA) on the NorSat-1 microsatellite and the Chinese meteorological satellite FY-3E/JTSIM mission, where a similar DARA instrument has been operated successfully since

2021. The DARA employs a three-cavity design with inverted aperture geometry to minimize stray light and a digital control electronics. DARA is calibrated and traceable to the WRR and SI standards (Montillet et al. 2026). Cavity B is the nominal channel and is operated continuously; cavity C is the back-up and is exposed once every 15 days; cavity A is the reference channel and is opened only rarely.

This work presents the first light results from DARA/PROBA-3 and compares these measurements with three established reference missions spanning the recent TSI record: an earlier version of the DARA on board of FY-3E/JTSIM metrological spacecraft (Zhu et al. 2025), VIRGO/PMO6 onboard of SOHO — the longest-running continuous TSI experiment (Finsterle et al. 2021), and the TSIS-1/TIM mission from LASP (Kopp 2016). Table 1 summarizes these missions and their key characteristics. It is important to underline that the records referenced to the WRR are converted to the SI scale, so that all four series are compared on a common scale in the following sections.

Section 2 describes the calibration used in space. Section 3 presents the first light measurements. Section 4 identifies the instrument-related outliers observed in the post-commissioning period. Section 5 cross-validates the resulting baseline with other data products derived from other missions (e.g., VIRGO/PMO6, TSIS-1/TIM). Section 6 concludes this study.

Table 1. TSI Missions, product versions and instruments used in this study. Note that the TSI scale is the original scale of the measurements for each radiometer.

Mission/Instrument	Version	Start Date	Status	Scale	Reference
VIRGO/PMO6 (SOHO)	v8	January 1996	Active	WRR	Finsterle et al. (2021)
DARA (FY-3E/JTSIM)	v1	July 2021	Active	WRR	Zhu et al. (2025)
TSIS-1/TIM	v4	November 2018	Active	SI	Kopp (2016)
DARA (PROBA-3)	v1	December 2024	Active	SI	This study

2. Calibration in Space

This section summarises the in-space calibration and resulting uncertainty budget of DARA-PROBA3. The pre-flight characterization, including the component-level calibration (aperture area, cavity reflectance, diffraction, lead-heating, electrical traceability) and the two system-level calibrations against the TRF at LASP and the WRR at PMOD/WRC, is described comprehensively by Montillet et al. (2026). The irradiances reported here are based on component-level calibration of Table 2. This native scale is SI-traceable through the calibration of the individual components.

Commissioning of the instrument began approximately four weeks after launch, once the OSC had reached the dedicated orbit and stable pointing configuration, and consisted of the exposure of the nominal DARA cavity (B) to sunlight in order to perform a preliminary check ahead of continuous measurements. Table 2

reports the resulting in-flight uncertainty budget for each cavity in irradiance mode under vacuum condition and referenced to the extraterrestrial solar spectrum. It also includes one term absent from the pre-flight budget of Montillet et al. (2026): the *Dark Correction*, discussed below.

During the commissioning phase, one of the main tasks is to perform the *Deep Space (DS)* measurements where the instrument is tilted by an approximate 70 deg. from the sun, such as the radiometer observes only the deep space. During these measurements, the cavity of the radiometers exchanges radiation with a different thermal background in the open-shutter state, when the cavity radiates to deep space, compared to the closed-shutter state when the cavity's thermal emission is reflected by the (gold-coated) backside of the shutter (Walter et al. 2017; Song et al. 2021; Montillet et al. 2026). The DS correction is then required to validate the numerical simulation of the thermal background effect, which is linked with the field-of-view and the temperature of the instruments.

Unlike the pre-flight background correction of Montillet et al. (2026), which was estimated from ground- and TRF-based measurements of the radiative exchange between the cavity and its immediate laboratory surroundings within a sealed tank, the dark correction reported here is derived from these DS measurements, and therefore reflects the thermal background encountered by the instrument on orbit. The resulting offsets are $-6.30\ \mathrm{W\,m^{-2}}$ (channel A), $-6.95\ \mathrm{W\,m^{-2}}$ (channel B), and $-6.10\ \mathrm{W\,m^{-2}}$ (channel C), corresponding to uncertainties of 135, 118, and 115 ppm, respectively. Propagating this term with the remaining component-level contributions raises the total combined standard uncertainty for each cavity to 181, 164, and 169 ppm (Channels A, B, C) compared to the pre-flight component-level budget of 149, 151 and 162 ppm reported by Montillet et al. (2026). This is expected: DS measurements performed in orbit yield substantially larger thermal background corrections than those inferred from the TRF's laboratory vacuum tank at ambient temperature.

3. First Light

3.1. First Light Values

On 25 February 2025, the instrument successfully passed the commissioning phase, and started recording the total solar irradiance. Channels A and C began at 10:35 UTC; channel A ran until 12:28 UTC and channel C until 14:29 UTC. Channel B began at 12:38 UTC and also ran until 14:29 UTC, so that channels A and B each cover approximately 2 h and channel C approximately 4 h. Figure 1 displays the observations recorded for each cavity. Channel A recorded a first TSI value of $1362.15\ \mathrm{W\,m^{-2}}$ (total uncertainty 187 ppm); channel B recorded $1362.02\ \mathrm{W\,m^{-2}}$ (168 ppm); and channel C recorded $1361.97\ \mathrm{W\,m^{-2}}$ (175 ppm). The scatter of the measurements of the individual cavities over their observation windows lies between 0.03 and $0.07\ \mathrm{W\,m^{-2}}$ and is mostly caused by solar variability. Cavities A and C, which overlap between 10:35 and 12:28 UTC, track each other closely; cavity B lies above cavity C by a constant offset over their common window. We observe an off-pointing episode which occurred between

Table 2. Corrections and calibrations used in space: DARA/PROBA3 characterization and calibration for irradiance in vacuum and with extra-terrestrial solar spectrum. The uncertainty (σ) is displayed in parts-per-million (ppm).

	Channel A		**Channel B**		**Channel C**	
Characterization item	Value	σ [ppm]	Value	σ [ppm]	Value	σ [ppm]
Aperture area [mm^2]	19.7011	92	19.6660	92	19.6842	91
Aperture temperature [°C]	19.99	24	19.99	24	19.99	24
Reflectance/absorptivity [ppm]	640	51	650	34	754	61
Diffraction (extra-terr. solar)	1.001279	25	1.001279	25	1.001279	25
Heater voltage	N/A	19	N/A	17	N/A	18
Shunt voltage	N/A	14	N/A	14	N/A	14
Shunt resistance [Ω]	429	40	422	40	433	40
Shunt resistor TCR [ppm/°C] +15°C to +45°C		10		10		10
Lead heating (vacuum)	1.000034	3	1.000044	4	1.000044	4
Dark correction [$W\,m^{-2}$]	6.30	135	6.95	118	6.10	115
Combined standard uncertainty		181		164		169

13:24 and 13:33 UTC, during the recording of cavities B and C. Cavity A had completed its run before it and is unaffected. The samples acquired during this time frame have been identified as outliers and removed. Note that all the first-light measurements reported here were recorded during the single orbit observed on 25 February 2025. The values reported above, and all the windowed means of Section 3.2, are computed from the remaining samples.

3.2. Comparison per Cavity

We extend the first light values of Section 3.1 to the full duration of each cavity's observation run (approximately 2 h for channels A and B and 4 h for channel C, all on 25 February 2025, spanning 10:35–14:29 UTC), treating each cavity independently, and not reporting a single whole-instrument average as Zhu et al. (2025). We compare these values against the two long-running reference missions, the VIRGO/PMO6 (v8 product, degradation-corrected, Finsterle et al. 2021 dataset Finsterle, Wolfgang 2026) and TSIS-1/TIM (v4, 6-hour average, Kopp 2016) time series. The VIRGO/PMO6 v8 product is referenced in SI scale. The WRR-to-SI correction was applied to the original measurements as described by Finsterle et al. (2021). For the same reason, the DARA-JTSIM observations were also corrected using the WRR-to-SI correction factor (Montillet et al. 2025). TSIS-1/TIM, itself SI-traceable via the TRF, is used without further correction (Kopp 2016).

For each channel, we compute the mean TSI value recorded by DARA-PROBA3 over its own recording window, and apply the same procedure to each reference series. The observations recorded by the DARA-JTSIM, VIRGO/PMO6, and TSIS-1/TIM are averaged over the identical period as the corresponding

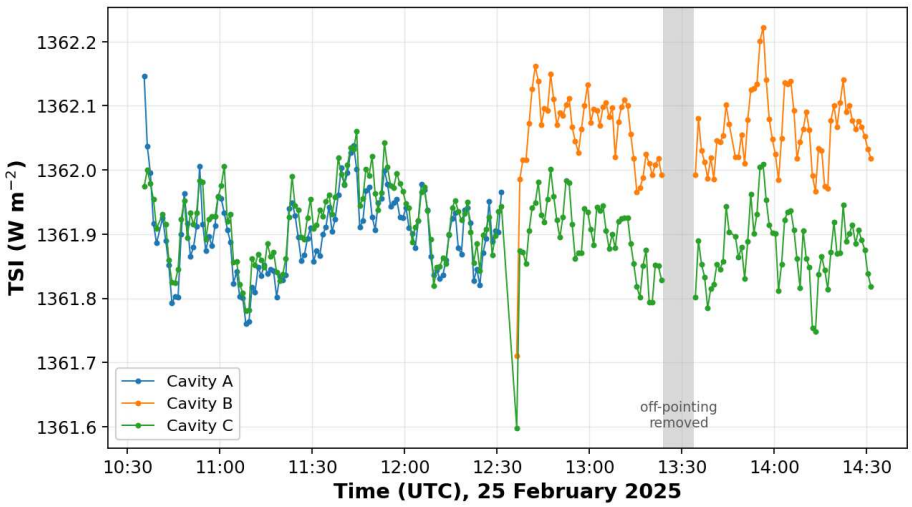


Figure 1. First light TSI time series recorded by the three DARA-PROBA3 cavities on 25 February 2025: Cavity A (blue, 10:35–12:28 UTC), Cavity B (orange, 12:38–14:29 UTC), and Cavity C (green, 10:35–14:29 UTC). The samples recorded during the off-pointing episode of 13:24–13:33 UTC have been removed.

DARA cavity. Table 3 reports for each channel, the resulting mean irradiance. In addition, it includes the mean and standard deviation of each series across the three cavities. DARA-PROBA3 exhibits the following values 1361.90, 1362.06, and 1361.90 W m^{-2} for cavities A, B, and C over their respective time windows. The mean value across the three cavities is 1361.96 W m^{-2} ($\sigma = 0.09$ W m^{-2}), in close agreement with the SI-corrected VIRGO/PMO6 mean over the same windows (1361.94 W m^{-2}, $\sigma = 0.01$ W m^{-2}), and 1.06 W m^{-2} below the TSIS-1/TIM mean (i.e. 1363.02 W m^{-2}, $\sigma = 0.01$ W m^{-2}). The DARA-JTSIM mean value (i.e. 1359.57 W m^{-2}, $\sigma = 0.03$ W m^{-2}) over the same time frame is 2.38 W m^{-2} below DARA-PROBA3 and 2.37 W m^{-2} below VIRGO/PMO6. Expressed as relative differences of the windowed means, the three cavities differ from VIRGO/PMO6 by 0.003 %, 0.009 % and 0.003 % (cavities A, B and C), which is within the scatter of the DARA-PROBA3 measurements. Against TSIS-1/TIM the same cavities are 0.081 %, 0.071 % and 0.082 % lower, and against DARA-JTSIM 0.173 %, 0.181 % and 0.172 % higher.

Because each instrument samples TSI at a different data rate, the same window-averaging procedure yields values of differing reliability depending on how well each instrument's own sampling resolves the window. The VIRGO/PMO6 measurements are sampled at 1-minute cadence, so its windowed average is a well-sampled estimate of the true mean TSI over that interval. Its low scatter across the three cavity windows (0.01 W m^{-2}) is evidence that TSI remained stable throughout the full 10:35–14:29 UTC period. TSIS-1/TIM is distributed as a 6-hour averaged product, so no window narrower than 6 h can be independently resolved from it. The windowed average reported here is therefore the value of the pre-averaged 6-hour bin(s) overlapping each cavity's window. The near-identical value obtained for all three cavities (i.e. mean value 1363.02 W m^{-2}, $\sigma = 0.01$)

reflects this product resolution. The main channel of the DARA-JTSIM records only ∼20 min of data per ∼101 min orbit, so its windowed average over a 2–4 h span is computed from only the sparse subset of samples that fall within that window; this reduces the effective number of independent measurements entering the average relative to VIRGO/PMO6 or DARA-PROBA3. Therefore, its channel-to-channel spread (mean 1359.57 $\mathrm{W\,m^{-2}}$, $\sigma = 0.03$) should be interpreted carefully with this reduced sampling (Montillet et al. 2025). DARA-PROBA3 itself is sampled continuously over each window at a 1-minute rate, so its own windowed average is, like the PMO6v8 product, fully resolved. Its spread across the three cavities (mean 1361.96 $\mathrm{W\,m^{-2}}$, $\sigma = 0.09\ \mathrm{W\,m^{-2}}$) reflects a stable offset between the cavities rather than the scatter introduced by the off-pointing episode, whose samples have been removed. Cavities A and C agree to within 0.01 $\mathrm{W\,m^{-2}}$, or 7 ppm, which is below the scatter of the individual measurements, while cavity B exceeds cavity C by 0.16 $\mathrm{W\,m^{-2}}$, or 117 ppm, an offset that is unchanged across the whole of the window they share. An offset of this magnitude remains within the combined standard uncertainty of a single cavity (see Table 2).

Table 3. First light value: TSI Measured from 10:35 to 14:29 UTC, on 25 February 2025. The last column displays the mean over the three cavity windows and the standard deviation (std) between them.

Instrument	Channel A	Channel B	Channel C	Mean ± std
DARA-PROBA3	1361.90	1362.06	1361.90	1361.96 ± 0.09
DARA-JTSIM	1359.55	1359.60	1359.57	1359.57 ± 0.03
VIRGO/PMO6	1361.94	1361.94	1361.95	1361.94 ± 0.01
TSIS-1/TIM	1363.01	1363.03	1363.03	1363.02 ± 0.01

4. Instrument-Related Outliers

Figure 2 presents the DARA-PROBA3 Cavity B record spanning from first light on 25 February 2025 through 10 October 2025. Outside a small number of discrete, localized excursion events, the record maintains a stable TSI baseline of ∼1360–1362 $\mathrm{W\,m^{-2}}$, consistent with the initial first-light values established in Section 3. It is important to note that the nominal channel (Cavity B) and the back-up channel (Cavity C) operate at different duty cycles. This asymmetric sampling is deliberate: by keeping Cavity C mainly closed in order to minimize the cumulative UV/EUV exposure that drives long-term radiometer degradation, allowing it to serve as a low-drift reference against which the nominal channel's performance can be tracked over time (Finsterle 2000). Degradation of the nominal channel will be assessed *a posteriori* from the ratio of its readings to those of the occasionally exposed back-up channel (Kopp 2025; Montillet et al. 2025). The interval covered by this first light study is too short for such an assessment, which is deferred to a later analysis of the mission record.

A close inspection of this near-continuous interval reveals that outliers fall into two distinct empirical categories, both directly linked to the spacecraft's orbital geometry and operations:

1. **Spacecraft Maneuvers (Type I):** Transient off-pointing events associated with formation-flying maintenance of the Occulter Spacecraft (OSC). These occur at a variable frequency—ranging from zero up to twice per 19-hour orbit—and have short durations bounded at ≤ 10 minutes.
2. **Perigee Fly-bys (Type II):** Excursions recorded during the perigee passage, when the Earth enters or approaches the instrument field of view. The proximity of the Earth perturbs several housekeeping parameters of the instrument—for example the temperatures across the sensor head and the electronics board, and the primary current measurement—so the affected samples are treated as unreliable and removed. These events repeat at the orbital cadence and exhibit longer durations ranging between 15 and 30 minutes, determined by the geometry of the trajectory near perigee.

To demonstrate the instrumental origin of the Type I and II outliers, we select a particular day, 2025-09-03, shown in Figure 3, on which two events are recorded: one Type I event near 15:00, and one Type II event near 10:30 UTC. Figure 4 displays the voltages from the four-quadrant (4Q) sun sensor for the same day. During the Type I event, the DARA pointing sensor (4-quadrant photo diode) show a variation of voltage across individual quadrants while the summed signal displays a small spike at $\approx$3.95 V, confirming a transient attitude motion relative to the solar disk rather than a genuine change in incident irradiance; the cavity's intrinsic voltage shows no comparable nudge during this event, indicating that the measurement remains undisturbed. During the Type II event, by contrast, the summed 4Q signal shows a drop consistent with the Earth entering or approaching the instrument field of view. This is linked with transient perturbations in several housekeeping parameters, for example the board temperatures and the primary current measurement, indicating that the fly-by disturbs the instrument in a different way from a manoeuvre. The instrument appears to continue measuring through the fly-by, so the affected samples are flagged and removed. Some of the housekeeping parameters for this day are shown in Figure 9 (Appendix B).

5. Cross-Validation With Other Data Products

To independently evaluate the TSI observation baseline, we compare the DARA-PROBA3 record with the continuous, minute-rate measurements of the PMO6v8 product. For the minute-rate comparison we restrict the analysis to the post-commissioning interval, from 1 August 2025 onwards, which provides a near-continuous record with substantially fewer commissioning- and manoeuvre-related outliers than the earlier part of the mission. The daily-averaged comparisons that follow cover the full record, from first light on 25 February 2025 to 10 October 2025.

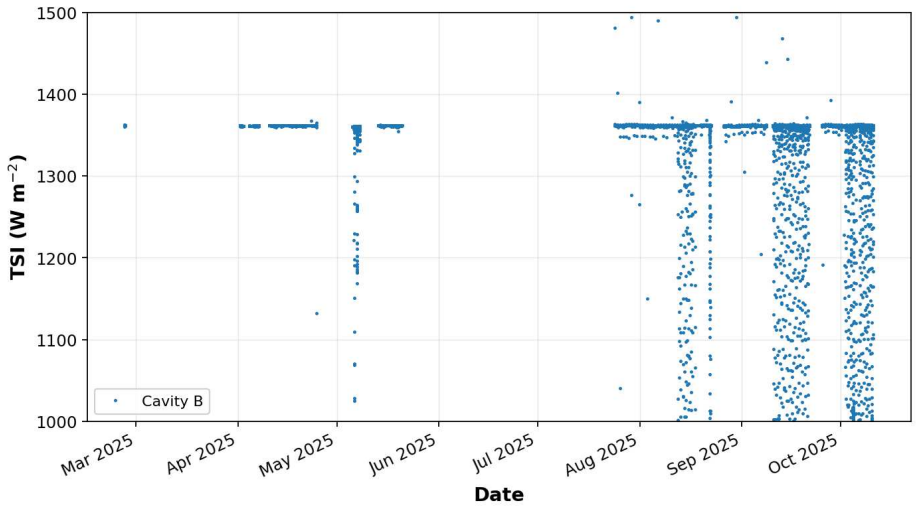


Figure 2. DARA-PROBA3 time series of TSI measurements from first light to 10 October 2025. As the Type I outliers can have very large scatter (up to ∼300 W m^{-2}), we reduced the scale of the figure.

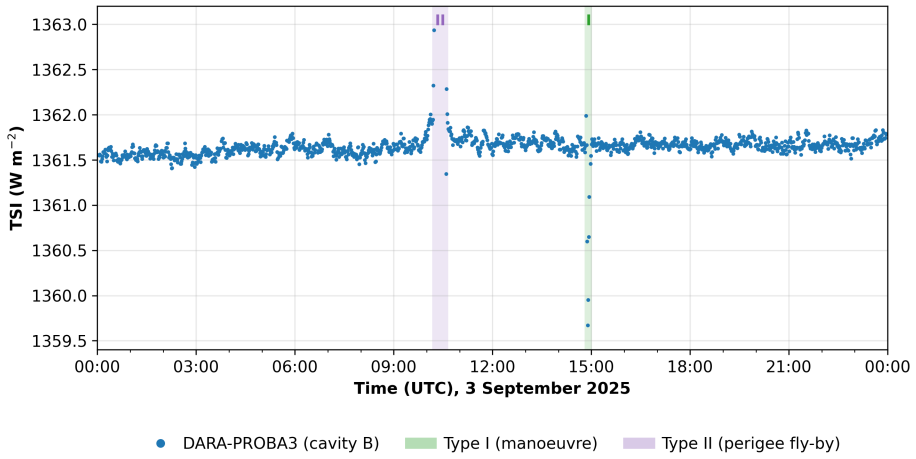


Figure 3. DARA-PROBA3 time series of TSI measurements on 2025-09-03, showing one Type I event near 15:00 and one Type II event near 10:30 UTC.

Figure 5 compares the minute-resolution time series of DARA-PROBA3 against the PMO6v8 product. At this resolution, DARA-PROBA3 reproduces the same short-timescale solar variability features recorded by PMO6v8, with the two baselines coincident to within 0.5 W m^{-2} throughout the interval shown. We next compare the daily-averaged DARA-PROBA3 (cavity B) and PMO6v8 time series over the full record (Figure 6). At this coarser resolution, the two series continue to track each other closely (below 0.15 W m^{-2}), additionally reproducing longer, multi-day dips and recoveries not readily visible at the minute scale,

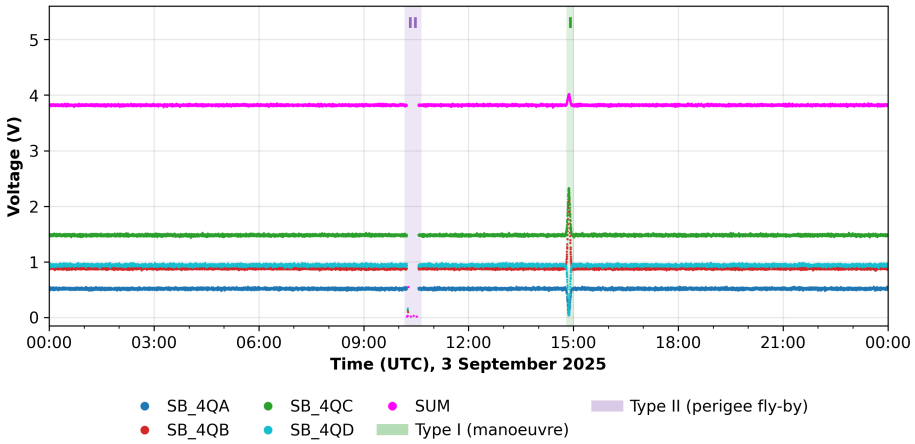


Figure 4. The voltage recorded by the four-quadrant (4Q) sun sensor, each quadrant in a different colour and the summed signal in magenta, on 2025-09-03. Near 15:00 UTC the individual quadrants swing while the summed signal shows a small spike, the signature of a Type I maneuver; near 10:30 UTC the summed signal itself drops, the signature of a Type II event.

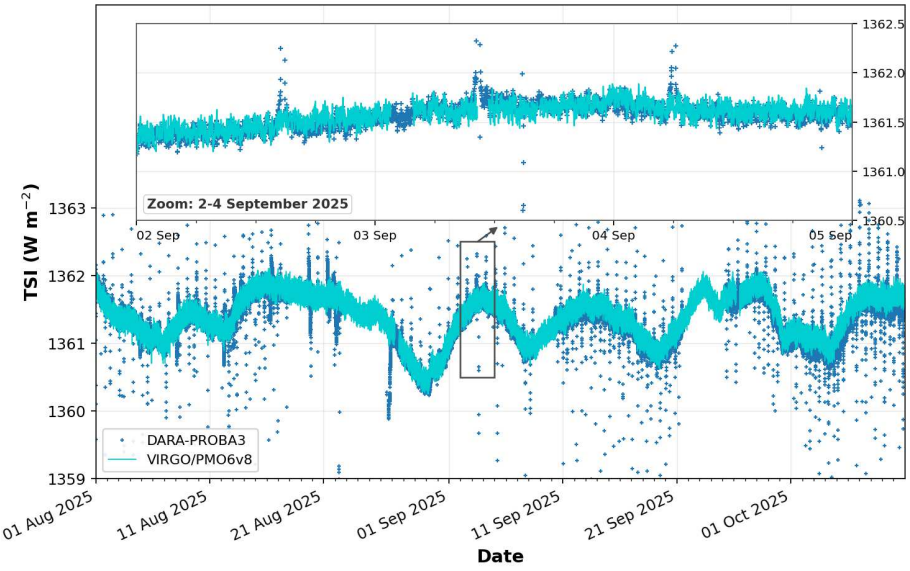


Figure 5. Comparison at minute rate between the PMO6v8 product (cyan) and the TSI observations recorded by DARA-PROBA3 (blue), from 1 August to 10 October 2025. The DARA-PROBA3 samples are shown unfiltered. A Zoom of a section of the time series is included at the top.

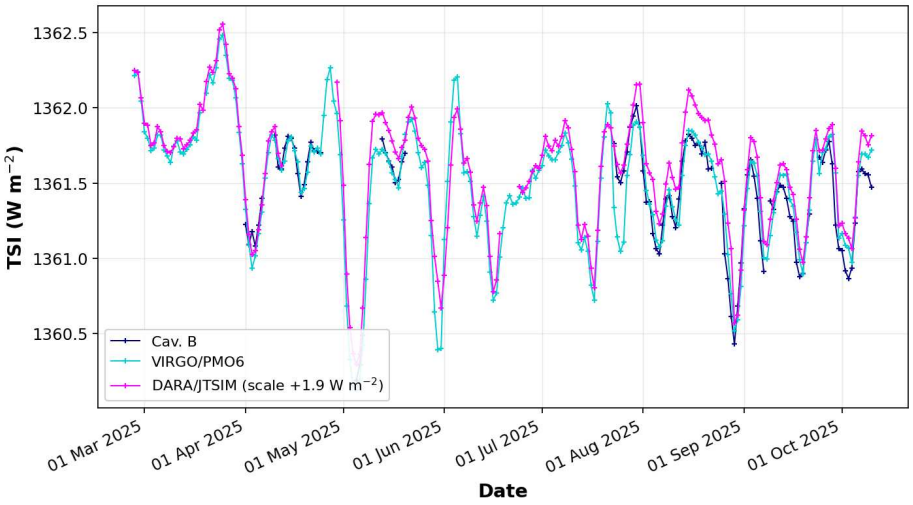


Figure 6. Comparison at daily rate between the PMO6v8 product, the TSI observations recorded by DARA-PROBA3 (cavity B) and DARA-JTSIM, over the full record from first light to 10 October 2025. The DARA-JTSIM series is shifted by +1.9 W m^{-2}.

confirming that DARA-PROBA3 resolves genuine solar-driven TSI variability consistent with PMO6v8 across both timescales. This close match between the irradiance recorded by the two instruments corroborates the results stated for the first light in Table 3. The daily-sampled DARA-JTSIM record shows the same sensitivity to solar fluctuations over this interval once its baseline is shifted by +1.9 W m^{-2}. This shift is smaller than the 2.38 W m^{-2} difference obtained at first light and close to the mean offset of 1.82 W m^{-2} between DARA-JTSIM and VIRGO/PMO6 reported over the JTSIM record by Montillet et al. (2025). The principal result of this comparison is therefore the close match between the DARA-PROBA3 and PMO6v8 baselines across the whole record, especially witnessed at daily resolution.

As an independent cross-check on the DARA-PROBA3 baseline, Figure 10 (Appendix) compares daily-averaged DARA-PROBA3 against the TSIS-1/TIM observations over the same full record, with TSIS-1/TIM offset by −1 W m^{-2} for visual clarity. The two series show the same sensitivity to solar fluctuations, providing an independent confirmation of the day-to-day PROBA3 baseline against a second SI-traceable reference, in addition to the PMO6v8 comparison above. The Section C (Appendix) gives more detailed comparison on the observations recorded by TSIS-1/TIM and the other radiometers selected in this study.

6. Conclusions

We have presented the first light results from the Digital Absolute Radiometer (DARA) onboard the ESA PROBA-3 mission, operated on its native component-level scale (Montillet et al. 2026). A Dark Correction derived from deep-space

measurements raised the combined standard uncertainty of Channels A, B and C to 181, 164 and 169 ppm.

First light was recorded on 25 February 2025, with Channels A, B, and C giving 1362.15, 1362.02, and 1361.97 $\mathrm{W\,m^{-2}}$, respectively, at their respective first-measurement epochs. The spread across cavities reflects a stable offset between Cavity B and Cavity C, consistent with the pre-flight characterisation from which the nominal and back-up channels were selected.

Extending the analysis from 25 February 2025 to 10 October 2025, we identified two distinct classes of instrumental outliers tied to the spacecraft's orbital geometry: short excursions associated with formation-flying maneuvers of the OSC, and longer excursions recorded during perigee fly-bys. The TSI observations recorded by the DARA-PROBA3 show close agreement with the PMO6v8 product from VIRGO/SOHO at both minute and daily-averaged resolution, correctly recording solar variability. The daily-sampled DARA-JTSIM and TSIS-1/TIM records show the same sensitivity to solar fluctuations over the same interval, although their absolute levels differ from that of DARA-PROBA3, DARA-JTSIM lying 2.38 $\mathrm{W\,m^{-2}}$ below and TSIS-1/TIM 1.06 $\mathrm{W\,m^{-2}}$ above.

To conclude, these results demonstrate that DARA-PROBA3 achieves an in-flight performance consistent with its pre-flight calibration, and establish a validated baseline against which the longer-term stability, degradation, and calibration of the instrument can be assessed as the PROBA-3 mission continues.

Acknowledgements J.-P.M., W.F., and M.H. gratefully acknowledge the support from the Karbacher-Funds. J.-P.M. also thanks the Swiss Space Office for support via the PRODEX funds. This research was supported by the International Space Science Institute (ISSI) in Bern, through ISSI International Team project 500 (Towards Determining the Earth Energy Imbalance from Space).

Appendix

A. The DARA-PROBA3 Instrument

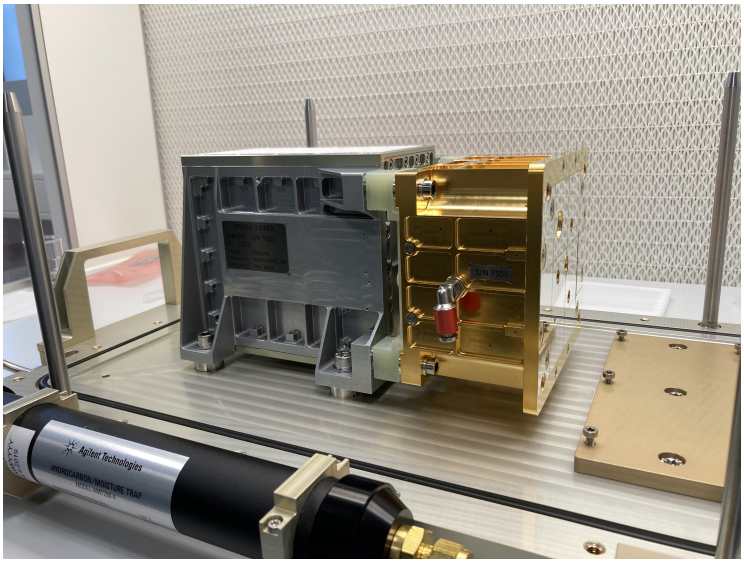


Figure 7. The DARA-PROBA3 flight model during pre-flight testing. The three circular openings in the front plate are the corresponding view-limiting apertures for each cavity.

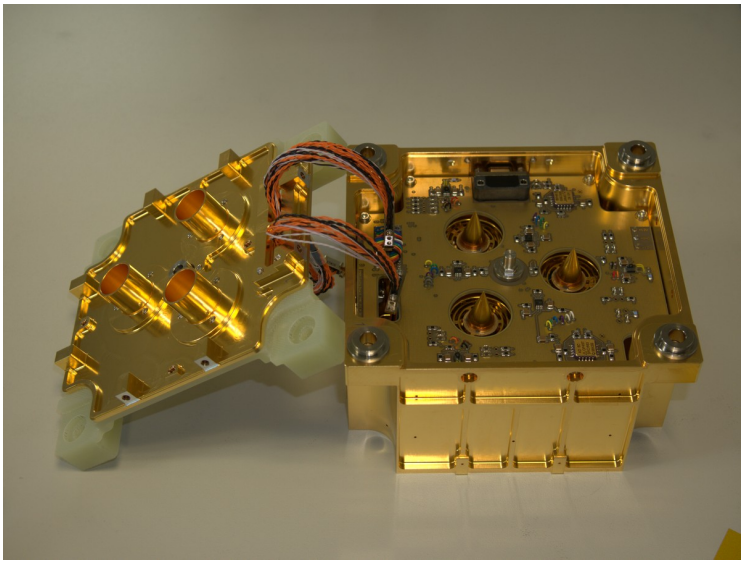


Figure 8. Interior of the head of DARA-PROBA3, which houses the cavities. On the right–hand side, we observe the three cavities arranged in a triangle. Each cavity exposes the conical interior.

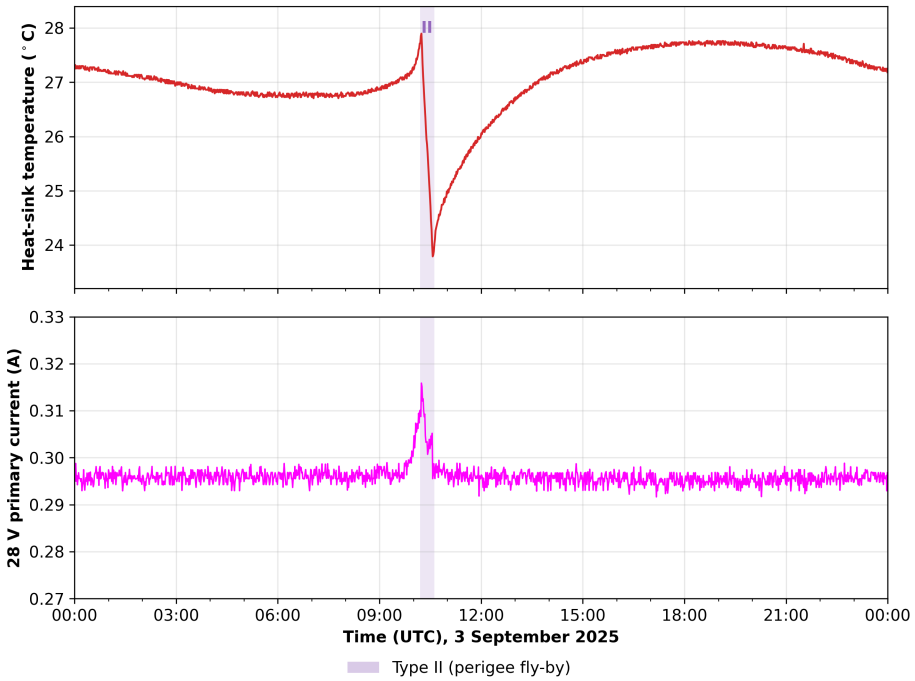


Figure 9. Housekeeping telemetry on 2025-09-03, on the same time axis as Figures 3 and 4. Top: cavity heat-sink temperature. Bottom: 28 V primary current. The purple band marks the Type II perigee fly-by (10:12–10:37 UTC).

B. Housekeeping Signature of a Perigee Fly-by

Figure 9 illustrates the disturbance on some housekeeping parameters related to the Type II perigee fly-by on 2025-09-03, the same day shown in Figures 3 and 4. During the fly-by the cavity heat-sink temperature rises to 27.9 °C at 10:14 UTC, drops by about 4 °C to 23.8 °C at 10:34 UTC, and then recovers over the following hours as nominal pointing is restored. The 28 V primary current shows a coincident excursion, rising from a baseline of 0.296 A to 0.316 A at 10:14 UTC. These perturbations confirm that the fly-by disturbs several housekeeping parameters of the instrument. The TSI observations recorded during this time are therefore removed.

C. Comparison with TSIS-1/TIM

The agreement in sensitivity described above in Section 5 does not extend to the absolute level. Over the first light windows DARA-PROBA3 lies 1.06 W m^{-2} below TSIS-1/TIM, a difference larger than the combined standard uncertainty of a single cavity. A comparable difference exists between the two reference records themselves: Montillet et al. (2025) report record-length means of 1361.40 W m^{-2} for VIRGO/PMO6 and 1362.48 W m^{-2} for TSIS-1/TIM, an offset of 1.08 W m^{-2}.

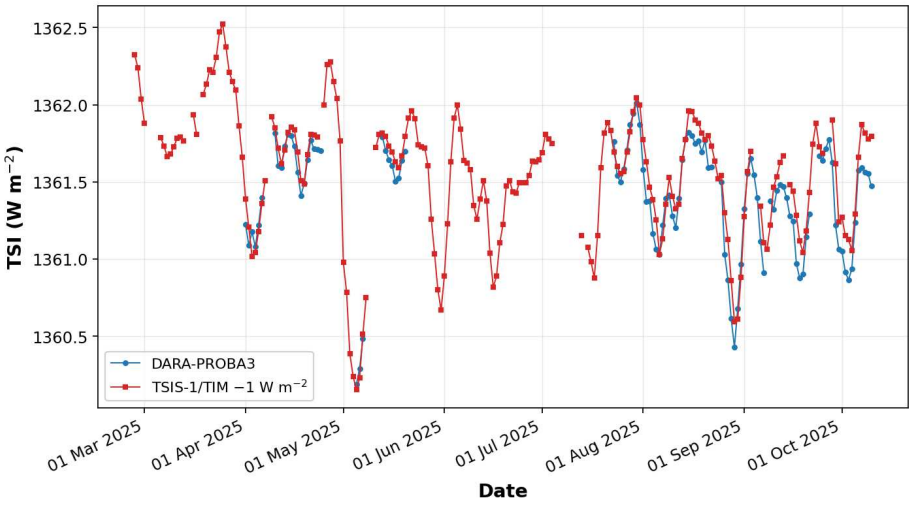


Figure 10. Daily-averaged TSI comparison between DARA-PROBA3 and TSIS-1/TIM over the full record, 25 February to 10 October 2025. TSIS-1/TIM is offset by -1 W m^{-2} for visual clarity; this offset is unrelated to the WRR-to-SI correction applied elsewhere in this work, since TSIS-1/TIM is already SI-traceable via the TRF.

DARA-PROBA3 therefore falls on the VIRGO/PMO6 side of a difference between the two records that predates this mission.

Author Contribution Conceptualization, J.-P.M. (Jean-Philippe Montillet), W.F. (Wolfgang Finsterle) and M.H. (Margit Haberreiter); methodology, J.-P.M., W.F., D. P. (Daniel Pfiffner) and M.H.; software, J.-P.M. and W.F.; validation, all co-authors; formal analysis, all co-authors; investigation, all co-authors; resources, J.-P.M. and W.F.; data curation, J.-P.M.; writing—original draft preparation, J.-P.M., W.F. and M.H.; writing—review and editing, J.-P.M.; project administration, J.-P.M. and W.F.; funding acquisition, J.-P.M. and W.F. All authors have read and agreed to the published version of the manuscript.

Funding J.-P. Montillet, W. Finsterle, and M. Haberreiter gratefully acknowledge support from the Karbacher-Funds. J.-P. Montillet also thanks the Swiss Space Office for support via the PRODEX funds supporting the making of the DARA dataset.

Data Availability *TSIS-1/TIM time series* are downloaded from https://lasp.colorado.edu/home/sorce/data/tsi-data (last accessed 02 February 2026). *PMO6v8* is available at https://www.pmodwrc.ch/en/research-development/space/soho/ (last accessed 06 September 2026). The dataset has also been recently added to the open archive repository https://www.astromat.org (Finsterle, Wolfgang 2026). The DARA 6-hourly product (JTSIM-DARAv1) is released either via the PMOD website (https://www.pmodwrc.ch/en/research-development/space/fy-3e/ — see link to the ftp server) or via the open archive repository https://www.astromat.org. Note that the DARA-PROBA3 data will be released via the ESA heliosphere archive.

Declarations

Conflict of interest The authors declare that they have no conflicts of interest.

References

Egorova, T., Rozanov, E., Arsenovic, P., Peter, T., Schmutz, W.: 2018, Contributions of Natural and Anthropogenic Forcing Agents to the Early 20th Century Warming. *Front. Earth Sci.* **6**, 206. DOI.

Eyring, V., Bony, S., Meehl, G.A., Senior, C.A., Stevens, B., Stouffer, R.J., Taylor, K.E.: 2016, Overview of the Coupled Model Intercomparison Project Phase 6 (CMIP6) experimental design and organization. *Geoscientific Model Development* **9**, 1937. DOI.

Fehlmann, A.: 2011, Metrology of Solar Irradiance. PhD thesis, University of Zurich. DOI.

Fehlmann, A., Kopp, G., Schmutz, W., Winkler, R., Finsterle, W., Fox, N.: 2012, Fourth World Radiometric Reference to SI radiometric scale comparison and implications for on-orbit measurements of the total solar irradiance. *Metrologia* **49**, S34. DOI.

Finsterle, W.: 2000, Helioseismology with VIRGO data: the search for solar G modes. PhD thesis, ETH Zurich. DOI.

Finsterle, W., Montillet, J.P., Schmutz, W., Sikonja, R., Kolar, L., Treven, L.: 2021, The total solar irradiance during the recent solar minimum period measured by SOHO/VIRGO. *Scientific Reports* **11**, 10. DOI.

Finsterle, Wolfgang: 2026, *PMO6v8 - Total Solar Irradiance Dataset from VIRGO/PMO6 - August 2026, Version 1.0*, Astromaterials Data Archive. DOI.

Hansen, J., Sato, M., Kharecha, P., von Schuckmann, K.: 2011, Earth's energy imbalance and implications. *Atmos. Chem. Phys* **11**, 13421. DOI.

Kopp, G.: 2016, Magnitudes and timescales of total solar irradiance variability. *J. Space Weather Space Clim.* **6**, A30. DOI. ADS.

Kopp, G.: 2025, Solar irradiance measurements. *Living Rev. Sol. Phys.* **22**, 1. DOI.

Kopp, G., Heuerman, K., Harber, D., Drake, G.: 2007, The TSI Radiometer Facility: absolute calibrations for total solar irradiance instruments. In: Butler, J.J., Xiong, J. (eds.) *Earth Observing Systems XII* **6677**, SPIE, 667709. International Society for Optics and Photonics. DOI.

Montillet, J.-P., Finsterle, W., Zhu, P., Haberreiter, M., Koller, S., Pfiffner, D., Wu, D., Ye, X., Yang, W. D.and Fang, et al.: 2025, Assessment of Instrument Performance of the FY3E/JTSIM/DARA Radiometer Through the Analysis of TSI Observations. *Remote Sens.* **17**, 3902. DOI.

Montillet, J.-P., Schmutz, W., Finsterle, W., Haberreiter, M., Kopp, G., Koller, S., Pfiffner, D., Vermeirssen, J., Gyo, M., Soder, R., Gander, M., Beeler, L., Spescha, M., Schlatter, P., Heuerman, K.: 2026, The DARA-PROBA3 radiometer: results from the pre-flight calibration campaign. *Metrologia* **63**, 035002. DOI.

Prša, A., Harmanec, P., Torres, G., Mamajek, E., Asplund, M., Capitaine, N., Christensen-Dalsgaard, J., Depagne, É., Haberreiter, M., Hekker, S., Hilton, J., Kopp, G., Kostov, V., Kurtz, D.W., Laskar, J., Mason, B.D., Milone, E.F., Montgomery, M., Richards, M., Schmutz, W., Schou, J., Stewart, S.G.: 2016, Nominal Values for Selected Solar and Planetary Quantities: IAU 2015 Resolution B3. *Astron. J.* **152**, 41. DOI.

Schmutz, W.: 2021, Changes in the Total Solar Irradiance and climatic effects. *J. Space Weather Space Clim.* **11**. DOI.

Schmutz, W., Fehlmann, A., Finsterle, G. W.and Kopp, Thuillier, G.: 2013, Total solar irradiance measurements with PREMOS/PICARD. In: Cahalan, R.F., Fischer, J. (eds.) *Radiation Processes in the Atmosphere and Ocean (IRS2012)*, *AIP Conference Series* **1531**, American Institute of Physics, 624. DOI.

Song, B., Ye, X., Finsterle, W., Gyro, M., Gander, M., Oliva, A.R., Pfiffner, D., Zhao, Y., Fang, W.: 2021, The Fengyun-3E/Joint Total Solar Irradiance Absolute Radiometer: Instrument Design, Characterization, and Calibration. *Sol. Phys.* **296**, 52. DOI.

Suter, M.: 2014, Advances in solar radiometry PhD Thesis. PhD thesis, University of Zurich.

Thuillier, G., Dewitte, S., Schmutz, W., Picard Team: 2006, Simultaneous measurement of the total solar irradiance and solar diameter by the PICARD mission. *Adv. Space Res.* **38**, 1792. DOI.

Walter, B., Levesque, P.-L., Kopp, G., Andersen, B., Beck, I., Finsterle, W., Gyo, M., Heuerman, K., Koller, S., Mingard, N., Remesal Oliva, A., Pfiffner, D., Soder, R., Spescha, M., Suter, M., Schmutz, W.: 2017, The CLARA/NORSAT-1 solar absolute radiometer: instrument design, characterization and calibration. *Metrologia* **54**, 674. DOI.

Zhu, P., Ye, X., Montillet, J.-P., Finsterle, W., Yang, D., Wu, D., Qi, J., Fang, W., Liu, H., Hu, X., Zhang, P.: 2025, The First Light From the Joint Total Solar Irradiance Mea-

surement Experiment Onboard the FY-3E Meteorological Satellite. *Earth Space Sci.* **12**, e2023EA003064. DOI.

Zhukov, A.N., Patel, B.D., Debrabandere, A., Dolla, L., Mierla, M., Shestov, S., Bourgoignie, B., Jean, C., Nicula, B., Talpeanu, D.-C., Zontou, Z., Fineschi, S., Gunár, S., Lamy, P., Peter, H., Rudawy, P., Tsinganos, K., Abbo, L., Aime, C., Andretta, V., Auchère, F., Berghmans, D., Beşliu-Ionescu, D., Gibson, S.E., Giordano, S., Heinzel, P., Inhester, B., Magdalenić, J., Marqué, C., Rodriguez, L., Steślicki, M., Zangrilli, L., Galano, D., Rougeot, R., Versluys, J., Thizy, C.: 2026, Ubiquitous Small-scale Dynamics in the Slow Solar Wind Formation Region Observed by Proba-3/ASPIICS. *Astrophys. J. Lett.* **999**, L41. DOI.